Journal of Biomolecular NMR, 4 (1994) 491–504
ESCOM



J-Bio NMR 192

# $^{1}H$ and $^{15}N$ resonance assignments and secondary structure of the carbon monoxide complex of sperm whale myoglobin

Yves Thériault[a,*], Thomas C. Pochapsky [a,**], Claudio Dalvit[a,***], Mark L. Chiu[b], Stephen G. Sligar[b] and Peter E. Wright[a,****]

[a]*Department of Molecular Biology, The Scripps Research Institute, La Jolla, CA 92037, U.S.A.*
[b]*Departments of Biochemistry and Chemistry, University of Illinois, Urbana, IL 61801, U.S.A.*

Received 16 September 1993
Accepted 28 January 1994

*Keywords:* Heme protein; Multidimensional NMR; Sequential assignment

## SUMMARY

Sequence-specific backbone $^{1}H$ and $^{15}N$ resonance assignments have been made for 95% of the amino acids in sperm whale myoglobin, complexed with carbon monoxide (MbCO). Many assignments for side-chain resonances have also been obtained. Assignments were made by analysis of an extensive series of homonuclear 2D spectra, measured with unlabeled protein, and both 2D and 3D $^{1}H$-$^{15}N$-correlated spectra obtained from uniformly $^{15}N$-labeled myoglobin. Patterns of medium-range NOE connectivities indicate the presence of eight helices in positions that are very similar to those found in the crystal structures of sperm whale myoglobin. The resonance assignments of MbCO form the basis for determination of the solution structure and for hydrogen-exchange measurements to probe the stability and folding pathways of myoglobin. They will also form a basis for assignment of the spectra of single-site mutants with altered ligand-binding properties.

## INTRODUCTION

Myoglobin (Mb) is a monomeric heme protein involved in oxygen storage in muscle. It is one of the most extensively studied proteins and is a paradigm for understanding structure–function relationships. Mb has been the subject of many X-ray and neutron diffraction structure determinations, detailed theoretical simulations, and numerous biochemical and spectroscopic investigations. Sperm whale (Springer and Sligar, 1987), human (Varadarajan et al., 1985), porcine (Dodson et al., 1988), and horse heart (Guillemette et al., 1991) myoglobins have been expressed

*Present address: Ontogen Corporation, Carlsbad, CA 92009, U.S.A.
**Present address: Department of Chemistry, Brandeis University, Waltham, MA 02254, U.S.A.
***Present address: Sandoz Pharma, CH-4002 Basel, Switzerland.
****To whom correspondence should be addressed.

in *Escherichia coli* and a large series of mutant proteins has been produced for detailed investigations of structure–function relationships (Braunstein et al., 1988; Lambright et al., 1989; Varadarajan et al., 1989; Carver et al., 1992; Gibson et al., 1992; Balasubramanian et al., 1993; Brantley et al., 1993).

Sperm whale Mb contains a single polypeptide chain of 153 amino acids and an iron protoporphyrin IX (heme) prosthetic group. High-resolution X-ray and neutron structures of sperm whale metMb (Takano, 1977a; Phillips et al., 1990), deoxyMb (Takano, 1977b), and of the oxygen (Phillips, 1980; Phillips and Schoenborn, 1981) and carbon monoxide complexes (Hanson and Schoenborn, 1981; Kuriyan et al., 1986) have been reported. Crystal structures of additional complexes of the sperm whale protein have been determined, together with structures of the human and porcine myoglobins. The dynamic properties of myoglobin have also been the subject of extensive experimental investigations (Frauenfelder et al., 1979; Hartmann et al., 1982; Phillips, 1990) and theoretical simulations (Levy et al., 1985; Elber and Karplus, 1987; Henry, 1993). Ligand binding is thought to be coupled to dynamic fluctuations in the protein structure (Case and Karplus, 1979; Kottalam and Case, 1988), since the X-ray and neutron structures of met- and deoxymyoglobin and its complexes with $O_2$ and CO reveal no open channels large enough to allow these diatomic ligands to enter or leave the heme pocket.

Understanding of the relationships between structure, dynamics and function of myoglobin would be greatly enhanced by the availability of detailed information on its 3D structure and backbone and side-chain dynamics in solution, both for the wild-type and mutant proteins. As a first step towards these goals, we have undertaken NMR studies of the diamagnetic carbon monoxide complex of sperm whale myoglobin. This paper reports sequence-specific assignments of the backbone resonances and many of the side-chain $^1H$ resonances of MbCO. Earlier work from this laboratory using 1D and 2D homonuclear NMR experiments, interpreted with the aid of the crystal structures, provided partial $^1H$ resonance assignments for a small number of protein side chains and for the heme (Mabbutt and Wright, 1985; Dalvit and Wright, 1987). In the present work, the NOE-based sequential assignment procedure (Billeter et al., 1982) was used to obtain assignments independently of prior knowledge of the 3D structure. This was made possible by the ability to express (Springer and Sligar, 1987) uniformly $^{15}N$-labeled sperm whale Mb for 2D and 3D $^{15}N$-dispersed NMR experiments. Unfortunately, the yield of labeled Mb from the minimal medium, containing glycerol as sole carbon source, required for expression was too low to allow economic labeling with $^{13}C$.

## MATERIALS AND METHODS

Sperm whale myoglobin (Sigma type II) was purified using previously described methods (Mabbutt and Wright, 1985). Wild-type myoglobin was also expressed, using the vector pCKR102 containing the *tac* - *lac* double promoter in *E. coli* strain NCM533, and purified as described previously (Springer and Sligar, 1987). Uniformly $^{15}N$-labeled protein was obtained by growing cells on medium containing glycerol (2.0 g/l) and 99% $^{15}N$-ammonium sulfate (2.3 g/l). Recombinant myoglobin differs from the native sperm whale protein in that it retains the initiator methionine at the N-terminus; however, this does not significantly affect the NMR spectrum. The carbon monoxide complex of myoglobin was prepared by reduction of a CO-saturated protein solution with solid sodium dithionite, followed by removal of excess reductant on a Sephadex

G-15 column (Mabbutt and Wright, 1985). Samples for NMR were prepared in potassium phosphate buffer (0.05 M, pH 5.6) in $D_2O$ or in 90% $H_2O$/10% $D_2O$. Freshly prepared samples of recombinant MbCO exhibited splitting of several resonances in the NMR spectra; this splitting was not observed in spectra of native sperm whale MbCO at pH 5.6 (Dalvit and Wright, 1987). After keeping the samples for 1–2 weeks, the extra resonances disappeared and spectra that were very similar to the native sperm whale protein were obtained. These slow, time-dependent spectral changes appear to be associated with reduction of an N-terminal methionine sulfoxide (Chiu, 1992); the spectra of the reduced form of the protein were used for assignment purposes. Except for the recombinant wild-type MbCO, spectra were also recorded for D122N, H64G and H64Y mutants. Only small resonance shifts near the sites of substitution were observed.

NMR spectra were recorded at 35 °C on Bruker AM and AMX spectrometers operating at $^1H$ frequencies of 500 and 600 MHz. All $^1H$ chemical shifts were referenced to the $Val^{68}$ $C^{\gamma}H_3$ resonance at −2.32 ppm relative to water at 4.68 ppm. $^{15}N$ chemical shifts were indirectly referenced to liquid $NH_3$ by using the $^1H$ frequency of the $H_2O$ resonance (Live et al., 1984; Bax and Subramanian, 1986). NMR data were processed on a CONVEX C-240 supercomputer using a modified version of FTNMR (Hare Research, Inc.). The 3D experiments were processed using FTNMR for the $\omega_1$ and $\omega_3$ planes and a separate routine, written by Dr. Mark Rance, for the $\omega_2$ Fourier transform.

Homonuclear 2D NMR spectra were recorded in the phase-sensitive mode with quadrature detection in the $\omega_1$ dimension, achieved using time-proportional phase incrementation (Drobny et al., 1979; Marion and Wüthrich, 1983). Double-quantum-filtered COSY spectra were recorded using standard pulse sequences and phase cycling (Rance et al., 1983). Relayed COSY spectra (Wagner, 1983) were acquired with various mixing times to optimize relayed coherence transfer for different spin systems. Double-quantum spectra (Braunschweiler et al., 1983; Rance and Wright, 1986) were recorded with multiple-quantum excitation periods of 22.5, 40, 60, 80 and 100 ms. NOESY spectra with mixing times of 60 and 100 ms were acquired using standard pulse sequences (Kumar et al., 1980), followed by a short Hahn-echo period to improve the quality of the baseline (Rance and Byrd, 1983; Davis, 1989). Suppression of the water resonance was accomplished by low-power presaturation. A NOESY spectrum with a mixing time of 200 ms was acquired using a 1,−1 observation pulse. In some cases a low-pass digital filter was applied prior to Fourier transformation to further reduce the residual water signal. Homonuclear 2D spectra were typically recorded with 2048 complex points in $t_2$ and 400–500 increments in $t_1$. Data were zero-filled to 2K × 4K complex points and appropriate window functions were applied before Fourier transformation. Window functions were typically Lorentzian/Gaussian in $t_2$ and exponential multiplication followed by sine-bell multiplication in $t_1$. Spectral widths were 8640 Hz or 10 kHz at 500 MHz and 10 or 12.5 kHz at 600 MHz.

Two-dimensional $^1H$-$^{15}N$-correlated spectra (HSQC, HSQC-NOESY and HSQC-TOCSY) were acquired using pulse sequences described previously (Bax et al., 1990; Norwood et al., 1990). $^{15}N$ decoupling was carried out with GARP-1 phase modulation (Shaka et al., 1985), and the DIPSI-2 sequence (Shaka et al., 1988) was used for isotropic mixing ($\tau$ = 24 ms) in HSQC-TOCSY experiments. HSQC-NOESY spectra were recorded with a mixing period of 100 ms. Water suppression was accomplished by low-power presaturation. Spectra were acquired with 2K complex points in $t_2$ and a spectral width of 6250 Hz; 512 $t_1$ increments were collected with a spectral width of 3048 Hz. A Gaussian window function was applied in $t_2$ and a cosine-bell

window function followed by a Lorentzian-to-Gaussian transformation was used in $t_1$.

Heteronuclear 3D TOCSY-HMQC and NOESY-HMQC spectra were acquired with mixing times of 24 and 100 ms, respectively, using similar pulse sequences to those described previously (Marion et al., 1989a,b; Driscoll et al., 1990; Fesik and Zuiderweg, 1990). The DIPSI-2 sequence was used for isotropic mixing and $^{15}N$ decoupling was achieved by application of GARP-1. The $^{15}N$-$^{1}H$ J coupling and refocusing delays were set to 2.3 ms. The water resonance was suppressed by low-power presaturation. The $t_1$, $t_2$ and $t_3$ dimensions were digitized by 256 × 64 × 1024 data points and had spectral widths of 7126, 3048 and 3112 Hz, respectively. The data were zero-filled to yield 512 × 64 × 1K real spectra after Fourier transformation. The window functions used were Lorentzian-to-Gaussian ($t_2$ and $t_3$), and cosine-bell followed by Lorentzian-to-Gaussian transformation ($t_1$).

## RESULTS AND DISCUSSION

Assignment of the MbCO NMR spectrum is complicated by the high degree of resonance overlap in this 153-amino acid protein and by the inefficiency of coherence transfer from the backbone NH protons to the side chain, due to the small $^{3}J_{HN\alpha}$ coupling constants and rapid $T_2$ relaxation associated with a helical protein of ~18 kDa molecular weight. Despite these

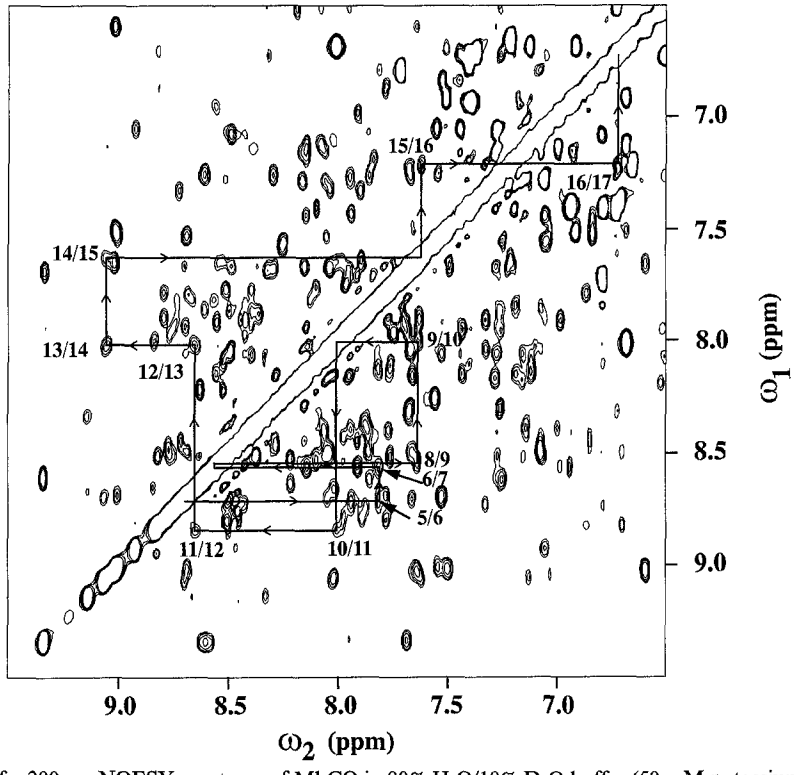


Fig. 1. Region of a 200-ms NOESY spectrum of MbCO in 90% $H_2O$/10% $D_2O$ buffer (50 mM potassium phosphate, pH 5.6) at 35 °C, showing amide–amide sequential NOEs. Sequential $d_{NN}$ NOE connectivities for part of the A-helix are indicated.

difficulties, the backbone proton resonances were assigned for all except six of the non-proline residues and extensive side-chain assignments were made using 2D homonuclear spectroscopy and 2D and 3D heteronuclear experiments with uniformly $^{15}$N-labeled myoglobin. Complete and unambiguous identification of all amino acid spin systems was not possible. Our assignment strategy relied upon identification of the relatively simple spin systems in homonuclear COSY, relayed COSY, double-quantum COSY and $^{1}$H-$^{15}$N TOCSY spectra (both 2D and 3D) as a starting point for application of standard sequential assignment procedures (Billeter et al., 1982). Most of the sequence-specific backbone assignments are supported by observation of multiple sequential and medium-range NOE connectivities and are thus considered to be highly reliable. In addition, parallel assignment work on the H64G and H64Y mutants (Pochapsky and Wright, unpublished data) helped to confirm the wild-type assignments in some cases by resolving overlaps and ambiguities in the sequential connectivities. During the sequential assignment procedure, NOE and TOCSY connectivities identified between backbone NH resonances and partial side-chain spin systems established on the basis of scalar connectivities were used to complete the spin system assignments wherever possible.

For several amino acid types, the spin systems could be identified completely prior to undertaking sequential assignment. The methods by which this can be achieved, using homonuclear COSY, relayed COSY, TOCSY, and multiple-quantum experiments, have been described in detail elsewhere (Chazin et al., 1988; Rance et al., 1989). Representative spectra, illustrating the excellent quality of the homonuclear 2D spectra of MbCO, have been published in earlier papers (Dalvit et al., 1986; Dalvit and Wright, 1987).

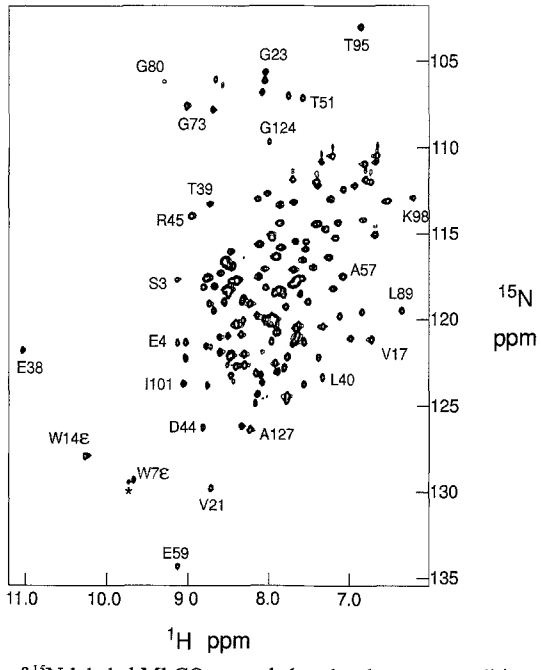


Fig. 2. $^{1}$H-$^{15}$N HSQC spectrum of $^{15}$N-labeled MbCO, recorded under the same conditions as the spectrum in Fig. 1. The asterisk indicates a peak arising from a small residual amount of protein containing the N-terminal methionine sulfoxide (see text).

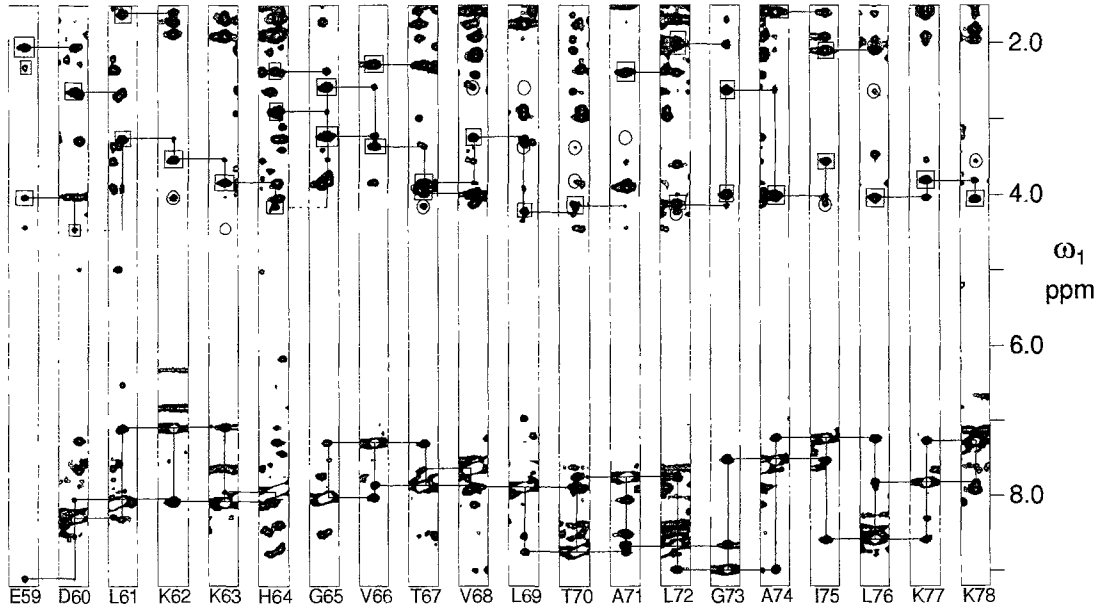


Fig. 3. Strips taken from the amide proton region of different $^{15}N$ planes of the 3D NOESY-HMQC spectrum of MbCO, arranged in sequential order. The figure illustrates the assignment of residues in the E-helix. The boxes, horizontal lines and circles indicate intraresidue, sequential and medium-range NOE connectivities, respectively. The dotted horizontal lines indicate $d_{\alpha N}$ NOEs that are observed at lower contour levels.

In the present analysis of the MbCO spectra, 10 of the 11 glycines were readily identified on the basis of the unique ($\omega_\alpha + \omega_{\alpha'}$ at $\omega_{NH}$) remote peak in a double-quantum spectrum in $H_2O$, recorded with excitation period $\tau_m = 22.5$ ms. Complete spin systems were also identified for all 17 alanines, three of the five threonines, and six of the eight valines, on the basis of scalar connectivities observed in double-quantum, relayed COSY, and TOCSY spectra. Double-quantum spectra with long excitation periods (60–100 ms) proved to be particularly valuable for identification of histidine spin systems by correlation of the $C^\delta H$ and $C^\varepsilon H$ resonances through the long-range coupling (Dalvit et al., 1987; Dalvit and Wright, 1987). For four histidines, additional $C^\delta H$-$C^\beta H$ correlations were observed in double-quantum spectra with long mixing times (Dalvit et al., 1987; Dalvit and Wright, 1987), providing unambiguous connections between the backbone AMX spin system and the imidazole ring. For a further five histidines, NOE connectivities were observed from the $C^\delta H$ resonance to the $C^\beta H$ and either the NH or $C^\alpha H$ resonances of the AMX spin system, leading to complete spin system identification. Assignment of all of the aromatic ring

→

Fig. 4. Summary of the sequential and medium-range NOE connectivities observed for MbCO. The asterisks indicate sequential NOE connectivities where a cross peak is present but is overlapped with another NOE connectivity. No attempt has been made to indicate the relative intensity of the NOE connectivities in this diagram. The location of the helices, based on the observed medium-range NOE connectivities, is shown. The CD loop (residues 44–49) exhibits NOE connectivities characteristic of a $3_{10}$-helix and is indicated by a broken 'helix' (see discussion in text). An ambiguous medium-range NOE connectivity between $Ala^{94}$ NH and either $Gln^{91}$ $C^\alpha H$ or $Ala^{90}$ $C^\alpha H$ is indicated by a broken line.

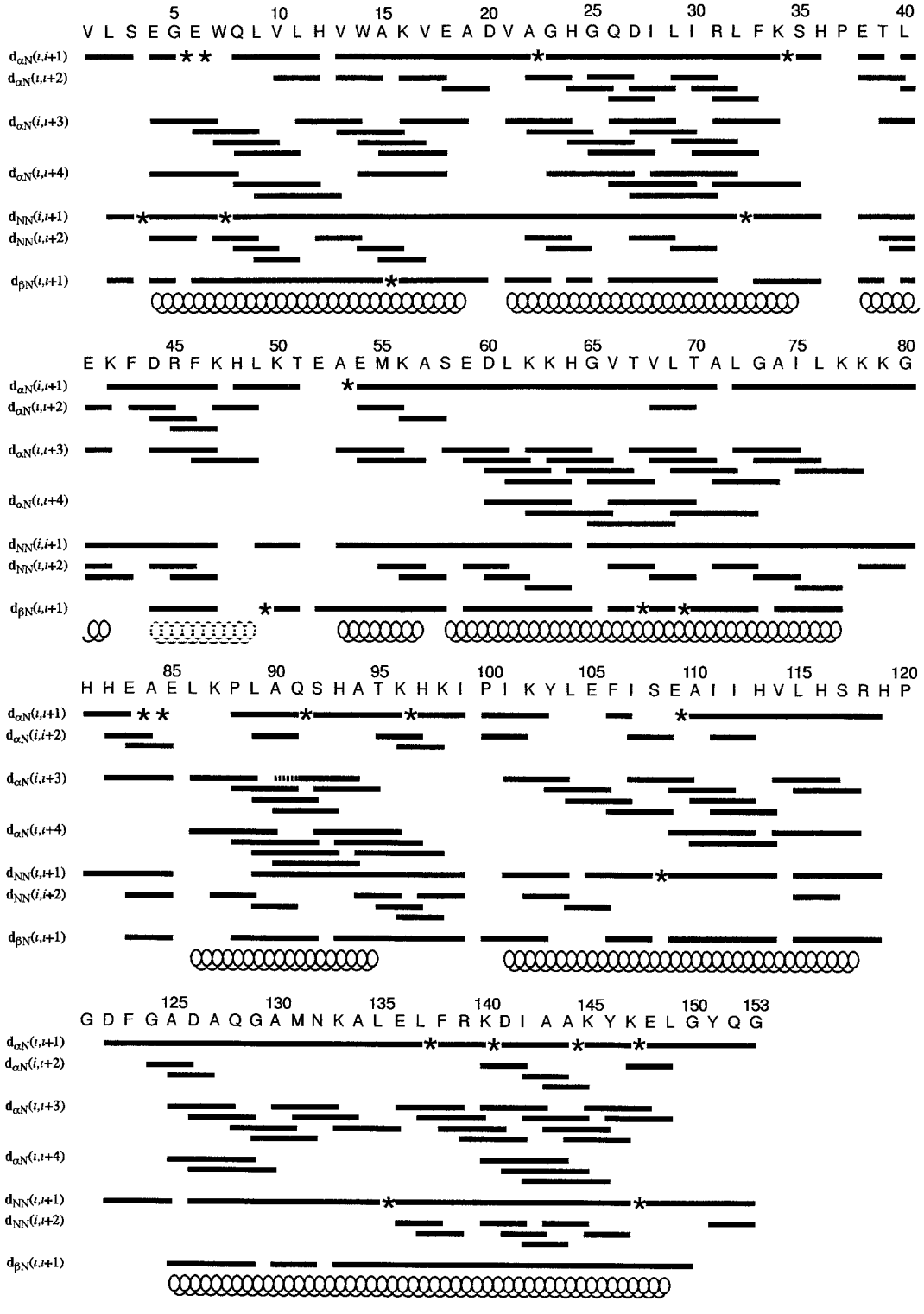
5 10 15 20 25 30 35 40
V L S E G E W Q L V L H V W A K V E A D V A G H G Q D I L I R L F K S H P E T L
$d_{\alpha N}(i,i+1)$
$d_{\alpha N}(i,i+2)$
$d_{\alpha N}(i,i+3)$
$d_{\alpha N}(i,i+4)$
$d_{NN}(i,i+1)$
$d_{NN}(i,i+2)$
$d_{\beta N}(i,i+1)$
45 50 55 60 65 70 75 80
E K F D R F K H L K T E A E M K A S E D L K K H G V T V L T A L G A I L K K K G
$d_{\alpha N}(i,i+1)$
$d_{\alpha N}(i,i+2)$
$d_{\alpha N}(i,i+3)$
$d_{\alpha N}(i,i+4)$
$d_{NN}(i,i+1)$
$d_{NN}(i,i+2)$
$d_{\beta N}(i,i+1)$
85 90 95 100 105 110 115 120
H H E A E L K P L A Q S H A T K H K I P I K Y L E F I S E A I I H V L H S R H P
$d_{\alpha N}(i,i+1)$
$d_{\alpha N}(i,i+2)$
$d_{\alpha N}(i,i+3)$
$d_{\alpha N}(i,i+4)$
$d_{NN}(i,i+1)$
$d_{NN}(i,i+2)$
$d_{\beta N}(i,i+1)$
125 130 135 140 145 150 153
G D F G A D A Q G A M N K A L E L F R K D I A A K Y K E L G Y Q G
$d_{\alpha N}(i,i+1)$
$d_{\alpha N}(i,i+2)$
$d_{\alpha N}(i,i+3)$
$d_{\alpha N}(i,i+4)$
$d_{NN}(i,i+1)$
$d_{NN}(i,i+2)$
$d_{\beta N}(i,i+1)$

protons has been made previously using multiple-quantum spectroscopy (Dalvit and Wright, 1987). The aromatic spin systems were connected to their backbone protons and $C^{\beta}H$ protons by means of NOEs.

Sequence-specific assignments were established by observation of networks of sequential $d_{\alpha N}$,$d_{NN}$ and $d_{\beta N}$ and, in the helical regions, medium-range $d_{\alpha N}(i,i+2)$, $d_{\alpha N}(i,i+3)$, $d_{\alpha N}(i,i+4)$, and $d_{NN}(i,i+2)$ NOE connectivities. The backbone and $C^{\beta}H$ proton resonances of spin systems that could be completely and unambiguously identified using the methods described above were used as starting points for the sequential assignments. The amide proton region of the homonuclear NOESY spectrum is fairly well resolved (Fig. 1) and considerable progress was made in assigning the helical regions using NOESY spectra acquired at different temperatures and pH values to permit resolution of overlapping cross peaks. However, it did not prove possible to complete the sequential assignments using the homonuclear data alone.

The availability of uniformly $^{15}N$-labeled Mb allowed us to use 2D and 3D $^{1}H$-$^{15}N$-correlated experiments to confirm and to extend the sequential assignments. The 2D $^{1}H$-$^{15}N$ HSQC spectrum of MbCO is shown in Fig. 2. The spectrum is reasonably well resolved, although some backbone amide cross peaks remain overlapped. Nevertheless, by using 3D NOESY-HMQC and TOCSY-HMQC spectra, in combination with the higher resolution 2D HSQC-NOESY and HSQC-TOCSY experiments, sequential NOE connectivities could be followed for most of the backbone. The 3D spectra proved particularly important for assignments, due to the greatly increased resolution. The TOCSY-HMQC spectrum was used to identify intraresidue connectivities from the amide proton resonance to the $C^{\alpha}H$, $C^{\beta}H$ and sometimes $C^{\gamma}H$ proton resonances. Sequence-specific assignments were then made by identifying networks of sequential $d_{\alpha N}(i,i+1)$, $d_{\beta N}(i,i+1)$ and $d_{NN}(i,i+1)$ NOE connectivities, supplemented by medium-range NOE connectivities in the helical regions. The sequential assignment of residues 59–78, which form the E-helix, is illustrated in Fig. 3. This figure shows strips taken from the amide proton region of different $^{15}N$ planes of the 3D NOESY-HMQC spectrum, arranged in sequential order. The boxes indicate intraresidue NOE connectivities, identified from the 2D or 3D $^{15}N$-edited TOCSY spectra or from homonuclear TOCSY spectra; the horizontal lines show sequential $d_{NN}$, $d_{\alpha N}$ and $d_{\beta N}$ NOE connectivities, and the circles indicate medium-range NOE connectivities. Multiple NOE connectivities are observed between all residues, giving confidence in the assignments.

A summary of the sequential and medium-range NOE connectivities obtained from the 3D NOESY-HMQC, 2D HSQC-NOESY and homonuclear NOESY spectra is given in Fig. 4 and the sequence-specific assignments made are listed in Table 1. The assignments in Table 1 are mostly supported by multiple sequential and medium-range NOE connectivities. Since $^{13}C$-labeled protein was not available and since $^{1}H$-$^{1}H$ TOCSY transfer is inefficient for a helical protein of ~18 kDa, complete side-chain proton assignments could not be made for all residues. Also, backbone $^{1}H$ and/or $^{15}N$ assignments are either missing or incomplete for eight residues ($Pro^{37}$, $His^{48}$, $Thr^{51}$, $Glu^{52}$, $Lys^{87}$, $Glu^{105}$, $Pro^{120}$ and $Gly^{121}$). Our inability to assign these backbone resonances at this time probably reflects the overlap that occurs even in the $^{15}N$-edited spectra, problems associated with rapid exchange of amide protons, and difficulties in observing connectivities to $C^{\alpha}H$ proton resonances under the water resonance. In the absence of $^{13}C$-labeled Mb, assignments could not be made for most of the proline residues.

The G-helix was the most difficult of the helical regions to assign. This was primarily due to near chemical-shift degeneracy of either the NH, $C^{\alpha}H$ or $^{15}N$ resonances of several pairs of

TABLE 1
$^{15}N$ AND $^{1}H$ CHEMICAL SHIFTS FOR RECOMBINANT MYOGLOBIN AT 35 °C AND pH 5.6

| Residue | $^{15}N$ | NH | $C^{\alpha}H$ | $C^{\beta}H$ | Others |
|---|---|---|---|---|---|
| Val[1a] | | | 4.31 | 2.15 | $C^{\gamma}H_3$ 0.91, 0.95 |
| Leu[2] | 126.2 | 8.35 | 4.51 | 0.66 | $C^{\gamma}H$ 1.13; $C^{\delta}H_3$ −0.37, 0.35 |
| Ser[3] | 117.7 | 9.14 | 4.59 | | |
| Glu[4] | 121.4 | 9.14 | 4.44 | 2.06[b], 2.23 | |
| Gly[5] | 106.0 | 8.66 | 3.87 | | |
| Glu[6] | 122.8 | 7.81 | 3.90 | 2.06[b], 2.33 | |
| Trp[7] | 119.0 | 8.56 | 4.58 | 3.12[b], 3.40[b] | $C^{\delta}H$ 6.97; $C^{\varepsilon 3}H$ 7.44; $C^{\zeta 3}H$ 7.06; $C^{\eta 2}H$ 7.28; $C^{\zeta 2}H$ 7.16; $N^{\varepsilon}H$ 9.67; $^{15}N^{\varepsilon}$ 129.4 |
| Gln[8] | 116.9 | 8.52 | 4.11 | 2.26 | |
| Leu[9] | 120.3 | 7.63 | 4.26 | 1.37 | $C^{\gamma}H$ 1.87; $C^{\delta}H_3$ 0.77, 0.84 |
| Val[10] | 120.3 | 8.00 | 3.70 | 2.66 | $C^{\gamma}H_3$ 0.90, 1.10 |
| Leu[11] | 118.1 | 8.81 | 4.29 | 1.66[b], 1.97 | $C^{\gamma}H$ 2.10; $C^{\delta}H_3$ 0.85, 0.95 |
| His[12] | 121.2 | 8.60 | 4.51 | 3.48 | $C^{\varepsilon}H$ 8.46; $C^{\delta}H$ 7.26 |
| Val[13] | 118.5 | 7.93 | 3.60 | 2.44 | $C^{\gamma}H_3$ 0.96, 1.19 |
| Trp[14] | 122.2 | 9.04 | 3.83 | 3.20, 3.44 | $C^{\delta}H$ 7.03; $C^{\varepsilon 3}H$ 7.13; $C^{\zeta 3}H$ 6.68; $C^{\eta 2}H$ 6.92; $C^{\zeta 2}H$ 7.51; $N^{\varepsilon}H$ 10.27; $^{15}N^{\varepsilon}$ 128.0 |
| Ala[15] | 118.6 | 7.61 | 4.14 | 1.45 | |
| Lys[16] | 115.4 | 7.17 | 3.84 | 1.46 | |
| Val[17] | 121.2 | 6.72 | 1.56 | 0.87 | $C^{\gamma}H_3$ −0.47, −0.10 |
| Glu[18] | 114.4 | 7.44 | 3.49 | 1.90 | |
| Ala[19] | 119.6 | 6.85 | 4.22 | 1.43 | |
| Asp[20] | 115.5 | 7.55 | 4.84 | 2.44, 2.84 | |
| Val[21] | 129.9 | 8.72 | 3.49 | 2.03 | $C^{\gamma}H_3$ 0.97, 0.97 |
| Ala[22] | 122.2 | 8.49 | 3.87 | 1.20 | |
| Gly[23] | 105.6 | 8.04 | 3.75, 3.83 | | |
| His[24] | 116.0 | 7.56 | 3.69 | 2.50, 2.69 | $C^{\varepsilon}H$ 7.91; $C^{\delta}H$ 6.28 |
| Gly[25] | 107.8 | 8.69 | 3.10, 3.27 | | |
| Gln[26] | 120.3 | 7.93 | 3.42 | 1.90 | |
| Asp[27] | 117.0 | 7.47 | 4.06 | 2.41, 2.57 | |
| Ile[28] | 119.8 | 8.16 | 3.31 | 1.52 | $C^{\gamma}H_2$ 0.97; $C^{\gamma}H_3$ 0.49; $C^{\delta}H_3$ 0.74 |
| Leu[29] | 118.2 | 7.20 | 3.00 | 0.17, 1.03 | $C^{\gamma}H$ 0.86; $C^{\delta}H_3$ −0.69, −0.29 |
| Ile[30] | 115.8 | 7.86 | 3.31 | 1.56 | $C^{\gamma}H_2$ 1.60; $C^{\gamma}H_3$ 0.74; $C^{\delta}H_3$ 0.49 |
| Arg[31] | 118.0 | 7.72 | 3.88 | | |
| Leu[32] | 122.6 | 7.92 | 3.94 | | $C^{\gamma}H$ 1.94; $C^{\delta}H_3$ 0.60, 0.96 |
| Phe[33] | 116.4 | 7.93 | 4.36 | 2.89, 2.97 | $C^{\delta}H$ 7.00; $C^{\varepsilon}H$ 6.46; $C^{\zeta}H$ 5.21 |
| Lys[34] | 116.7 | 8.56 | 4.03 | 1.73 | |
| Ser[35] | 113.0 | 8.15 | 4.02 | 3.41, 3.68 | |
| His[36] | 117.1 | 8.05 | 4.84 | 2.94 | $C^{\varepsilon}H$ 8.15; $C^{\delta}H$ 7.10 |
| Pro[37] | | | | | |
| Glu[38] | 121.8 | 11.03 | 4.48 | 2.74[b] | |
| Thr[39] | 113.3 | 8.73 | 4.19 | | $C^{\gamma}H_3$ 1.14[b] |
| Leu[40] | 123.4 | 7.32 | 3.85 | 1.02, 1.81 | $C^{\gamma}H$ 1.24; $C^{\delta}H_3$ −0.08, 0.47 |
| Glu[41] | 113.0 | 7.22 | 4.04 | | |
| Lys[42] | 113.2 | 7.69 | 4.07 | 2.28[b], 2.90 | |
| Phe[43] | 118.8 | 8.32 | 5.01 | 2.69, 3.29 | $C^{\delta}H$ 7.29; $C^{\varepsilon}H$ 6.07; $C^{\zeta}H$ 4.73 |
| Asp[44] | 126.4 | 8.83 | 4.28 | 2.74 | |
| Arg[45] | 114.0 | 8.98 | 4.12 | 1.12 | |

TABLE 1 (continued)

| Residue | $^{15}N$ | NH | $C^{\alpha}H$ | $C^{\beta}H$ | Others |
|---|---|---|---|---|---|
| Phe[46] | 112.3 | 7.07 | 5.11 | 2.29, 3.27 | $C^{\delta}H$ 6.76; $C^{\varepsilon}H$ 6.49; $C^{\zeta}H$ 6.58 |
| Lys[47] | 116.6 | 7.59 | 3.91 | | |
| His[48] | | | 3.91[b] | 3.04, 3.16 | $C^{\varepsilon}H$ 8.32; $C^{\delta}H$ 7.17 |
| Leu[49] | 123.9 | 7.54 | 4.04 | 1.92, 0.76 | $C^{\gamma}H$ 1.15; $C^{\delta}H_3$ 0.63, 0.87 |
| Lys[50] | 119.1 | 8.23 | 4.28 | 1.90 | |
| Thr[51] | 107.1 | 7.58 | | | $C^{\gamma}H_3$ 1.18[b] |
| Glu[52] | | | | | |
| Ala[53] | 120.1 | 8.33 | 3.94 | 1.34 | |
| Glu[54] | 117.9 | 7.66 | 3.92 | 1.94 | |
| Met[55] | 118.2 | 8.04 | 3.82 | 2.10[b] | $C^{\varepsilon}H_3$ 1.75 |
| Lys[56] | 118.5 | 8.49 | 3.63 | 1.72 | |
| Ala[57] | 117.5 | 7.08 | 4.23 | 1.40 | |
| Ser[58] | 110.9 | 6.81 | 4.44 | 3.87, 3.96 | |
| Glu[59] | 134.5 | 9.13 | 4.06 | 2.06, 2.34 | |
| Asp[60] | 119.0 | 8.35 | 4.48 | 2.66 | |
| Leu[61] | 123.7 | 8.08 | 3.28 | 0.72, 1.63 | $C^{\gamma}H$ 0.85; $C^{\delta}H_3$ −0.14, 0.47 |
| Lys[62] | 119.8 | 7.12 | 3.56 | 1.73[b] | |
| Lys[63] | 117.6 | 8.13 | 3.85 | 1.94[b] | |
| His[64] | 120.1 | 7.97 | 4.17 | 2.41, 2.91 | $C^{\varepsilon}H$ 7.13; $C^{\delta}H$ 4.92 |
| Gly[65] | 106.1 | 8.06 | 2.61, 3.24 | | |
| Val[66] | 120.4 | 7.32 | 3.38 | 2.30 | $C^{\gamma}H_3$ 0.87, 0.95 |
| Thr[67] | 123.1 | 7.89 | 3.84 | 4.01 | $C^{\gamma}H_3$ 1.50 |
| Val[68] | 121.2 | 7.66 | 3.26 | 0.86 | $C^{\gamma}H_3$ −2.32, −0.59 |
| Leu[69] | 116.4 | 7.91 | 4.25 | 1.47 | $C^{\gamma}H$ 1.76; $C^{\delta}H_3$ 0.62, 0.76 |
| Thr[70] | 117.7 | 8.79 | 4.18 | 4.46 | $C^{\gamma}H_3$ 1.43 |
| Ala[71] | 124.8 | 7.78 | 4.62 | 2.40 | |
| Leu[72] | 118.1 | 8.68 | 4.13 | 1.71[b], 2.03 | $C^{\gamma}H$ 1.15; $C^{\delta}H_3$ 0.42, 0.90 |
| Gly[73] | 107.6 | 9.02 | 2.64, 4.02 | | |
| Ala[74] | 121.4 | 7.56 | 4.06 | 1.62 | |
| Ile[75] | 116.4 | 7.26 | 3.58 | 2.12 | $C^{\gamma}H_3$ 0.82 |
| Leu[76] | 121.9 | 8.61 | 4.06 | 1.03[b], 1.96[b] | $C^{\gamma}H$ 1.45; $C^{\delta}H_3$ −0.14, 0.79 |
| Lys[77] | 113.3 | 7.86 | 3.84 | 1.60[b] | |
| Lys[78] | 114.7 | 7.30 | 4.08 | 1.83, 1.97 | |
| Lys[79] | 120.0 | 7.96 | 0.92 | | |
| Gly[80] | 106.1 | 9.31 | 3.24, 4.11 | | |
| His[81] | 122.3 | 7.36 | 4.84 | 3.07, 3.35 | $C^{\varepsilon}H$ 8.51; $C^{\delta}H$ 7.14 |
| His[82] | 114.2 | 6.82 | 5.32 | 2.78, 3.74 | $C^{\varepsilon}H$ 7.63; $C^{\delta}H$ 6.69 |
| Glu[83] | 123.8 | 8.75 | 3.97 | 1.99[b] | |
| Ala[84] | 118.2 | 8.52 | 4.03 | 1.38 | |
| Glu[85] | 117.8 | 8.40 | 4.06 | 2.23 | |
| Leu[86] | 124.8 | 8.18 | 3.97 | 2.37[b] | |
| Lys[87] | | | | | |
| Pro[88] | | | 4.29[c] | | $C^{\delta}H_2$ 3.51[c] |
| Leu[89] | 119.7 | 6.34 | 3.77 | 1.18, 1.47 | $C^{\gamma}H$ 0.58; $C^{\delta}H_3$ 0.29, 0.42 |
| Ala[90] | 120.8 | 8.34 | 3.44 | 1.19 | |
| Gln[91] | 114.4 | 7.86 | 3.56 | 1.90, 2.13 | |
| Ser[92] | 115.4 | 7.96 | 3.54 | | |
| His[93] | 121.5 | 7.70 | 2.55 | 1.77 | $C^{\varepsilon}H$ 1.63; $C^{\delta}H$ 1.11; $N^{\delta}H$ 9.38; $^{15}N^{\delta}$ 64.9 |

TABLE 1 (continued)

| Residue | $^{15}N$ | NH | $C^{\alpha}H$ | $C^{\beta}H$ | Others |
|---|---|---|---|---|---|
| $Ala^{94}$ | 119.3 | 7.79 | 3.11 | 0.30 | |
| $Thr^{95}$ | 103.0 | 6.85 | 3.85 | 4.01 | $C^{\gamma}H_3$ 0.99 |
| $Lys^{96}$ | 121.3 | 7.00 | 4.23 | 0.99, 1.18 | |
| $His^{97}$ | 114.7 | 7.14 | 4.24 | 1.65[b], 2.75[b] | $C^{\varepsilon}H$ 8.54; $C^{\delta}H$ 2.34 |
| $Lys^{98}$ | 112.8 | 6.19 | 3.27 | 1.92 | |
| $Ile^{99}$ | 120.1 | 7.92 | 4.40 | 1.40 | |
| $Pro^{100}$ | | | 4.44[b] | | |
| $Ile^{101}$ | 123.8 | 9.06 | 3.56 | 1.84 | $C^{\gamma}H_2$ 1.23, 1.30; $C^{\gamma}H_3$ 0.77; $C^{\delta}H_3$ 0.22 |
| $Lys^{102}$ | 119.6 | 8.69 | 3.94 | 1.43, 1.79 | |
| $Tyr^{103}$ | 115.5 | 7.67 | 4.52 | | $C^{\delta}H$ 7.30; $C^{\varepsilon}H$ 7.20 |
| $Leu^{104}$ | 120.0 | 8.06 | 5.03 | 2.41 | $C^{\gamma}H$ 1.90; $C^{\delta}H_3$ 0.73, 1.08 |
| $Glu^{105}$ | | | | | |
| $Phe^{106}$ | 118.5 | 7.81 | 4.81 | 2.94, 3.52[b] | $C^{\delta}H$ 6.81; $C^{\varepsilon}H$ 7.44; $C^{\zeta}H$ 7.44 |
| $Ile^{107}$ | 119.1 | 8.74 | 4.39 | 2.16 | $C^{\gamma}H_2$ 1.39, 1.46; $C^{\gamma}H_3$ 1.02; $C^{\delta}H_3$ 0.31 |
| $Ser^{108}$ | 120.8 | 7.89 | 4.50 | | |
| $Glu^{109}$ | 120.8 | 7.92 | 4.12 | 2.40[b] | |
| $Ala^{110}$ | 122.2 | 7.77 | 4.15 | 1.60 | |
| $Ile^{111}$ | 117.8 | 8.40 | 3.48 | | |
| $Ile^{112}$ | 118.3 | 7.87 | 3.72 | 2.25 | $C^{\gamma}H_3$ 1.14 |
| $His^{113}$ | 117.9 | 8.46 | 4.27 | 3.22, 3.30 | $C^{\varepsilon}H$ 8.00; $C^{\delta}H$ 6.82 |
| $Val^{114}$ | 120.3 | 8.43 | 3.61 | 2.02 | $C^{\gamma}H_3$ 0.98[e] |
| $Leu^{115}$ | 120.4 | 8.39 | 3.75 | 1.34 | $C^{\gamma}H$ 1.77; $C^{\delta}H_3$ 0.51, 0.69 |
| $His^{116}$ | 115.7 | 8.13 | 4.32 | 3.34 | $C^{\delta}H$ 7.45; $C^{\varepsilon}H$ 8.46 |
| $Ser^{117}$ | 112.6 | 8.00 | 3.90 | 3.74 | |
| $Arg^{118}$ | 115.8 | 8.13 | 3.87 | 1.14 | $C^{\delta}H_2$ 2.55; $^{15}N^{\varepsilon}$ 96.9; $N^{\varepsilon}H$ 6.66 |
| $His^{119}$ | 114.6 | 7.40 | 5.23 | 3.14, 3.24 | $C^{\varepsilon}H$ 8.61; $C^{\delta}H$ 6.92 |
| $Pro^{120}$ | | | | | |
| $Gly^{121}$ | | | | | |
| $Asp^{122}$ | 117.7 | 7.58[d] | 5.02[d] | 2.40, 2.80[d] | |
| $Phe^{123}$ | 123.3 | 8.11[e] | 5.01[e] | 2.71, 3.36[e] | $C^{\delta}H$ 7.10; $C^{\varepsilon}H$ 7.32; $C^{\zeta}H$ 7.19 |
| $Gly^{124}$ | 109.6 | 8.00 | 3.85, 4.31 | | |
| $Ala^{125}$ | 121.0 | 8.51 | 3.77 | 1.39 | |
| $Asp^{126}$ | 117.4 | 8.60 | 4.29 | 2.53, 2.66 | |
| $Ala^{127}$ | 126.5 | 8.24 | 3.97 | 1.52 | |
| $Gln^{128}$ | 118.4 | 8.55 | 3.41 | 1.73[b] | |
| $Gly^{129}$ | 106.8 | 8.08 | 3.87 | | |
| $Ala^{130}$ | 124.4 | 7.77 | 3.93 | 1.51 | |
| $Met^{131}$ | 116.5 | 8.54 | 4.47 | 2.36 | $C^{\varepsilon}H_3$ 2.25 |
| $Asn^{132}$ | 117.6 | 8.75 | 4.47 | 2.90, 2.99 | $^{15}N^{\varepsilon}$ 112.32; $N^{\varepsilon}H$ 6.93, 7.39 |
| $Lys^{133}$ | 120.1 | 7.94 | 4.06 | 1.84 | |
| $Ala^{134}$ | 122.6 | 8.41 | 3.85 | 1.40 | |
| $Leu^{135}$ | 116.1 | 8.48 | 4.39 | 1.63[b] | |
| $Glu^{136}$ | 123.2 | 8.47 | 3.87 | 2.22 | |
| $Leu^{137}$ | 122.0 | 8.30 | 4.08 | 1.56 | $C^{\gamma}H$ 1.80; $C^{\delta}H_3$ 1.10, 1.23 |
| $Phe^{138}$ | 118.3 | 7.87 | 4.04 | 3.29, 3.50[b] | $C^{\delta}H$ 7.09; $C^{\varepsilon}H$ 7.14; $C^{\zeta}H$ 6.99 |
| $Arg^{139}$ | 116.9 | 8.46 | 3.47 | 1.61[b] | |
| $Lys^{140}$ | 121.6 | 8.78 | 3.90 | 2.00 | |
| $Asp^{141}$ | 122.1 | 8.47 | 3.89 | 2.52, 2.71 | |

TABLE 1 (continued)

| Residue | $^{15}N$ | NH | $C^{\alpha}H$ | $C^{\beta}H$ | Others |
|---|---|---|---|---|---|
| Ile[142] | 122.7 | 8.30 | 3.37 | 1.27 | $C^{\gamma}H_2$ 0.56, 0.73; $C^{\gamma}H_3$ −0.03; $C^{\delta}H_3$ −0.13 |
| Ala[143] | 123.2 | 8.16 | 3.58 | 1.39 | |
| Ala[144] | 120.6 | 7.65 | 4.14 | 1.55 | |
| Lys[145] | 119.0 | 7.53 | 4.13 | 1.96 | |
| Tyr[146] | 121.4 | 9.03 | 3.87 | 3.06[b], 3.48 | $C^{\delta}H$ 6.60; $C^{\epsilon}H$ 6.41 |
| Lys[147] | 117.7 | 7.64 | 4.06 | 1.94 | |
| Glu[148] | 121.0 | 7.64 | 4.01 | 2.19 | |
| Leu[149] | 117.1 | 7.70 | 4.18 | 1.40, 1.74 | $C^{\gamma}H$ 1.74; $C^{\delta}H_3$ 0.53, 0.76 |
| Gly[150] | 107.0 | 7.75 | 3.69, 4.04 | | |
| Tyr[151] | 121.4 | 7.96 | 4.53 | 2.43 | $C^{\delta}H$ 6.47; $C^{\epsilon}H$ 6.41 |
| Gln[152] | 124.3 | 8.19 | 4.06 | 1.81, 2.01 | $C^{\gamma}H_2$ 2.26 |
| Gly[153] | 113.1 | 6.53 | 3.43, 3.50 | | |

[a] The recombinant sperm whale myoglobin contains a Met[0] residue for which no assignment was obtained. The presence of Met[0] influences the chemical shifts of Val[1], which are at 3.82 ppm for the α- and 2.37 ppm for the β-proton resonances in native sperm whale myoglobin.

[b] Assignments based on a combination of intraresidual and sequential NOEs.

[c] Tentative assignments based on NOEs to the amide proton of Leu[89].

[d] In the Asn[122] mutant, the chemical-shift values are respectively 7.77, 5.02, 2.94 and 2.40 ppm for the Asn[122] resonances.

[e] The chemical shifts in the Asn[122] mutant are respectively 8.16, 4.94 and 3.30 ppm.

sequentially adjacent amino acids. The 2D HSQC-NOESY spectrum, with its higher digital resolution, proved to be helpful for resolving the NOE connectivities between these residues. Sequential side chain–backbone or side chain–side chain NOEs were also particularly important for making assignments for the G-helix. The availability of the H64G mutant proved to be useful for confirming the assignments for the G-helix, since the near degeneracy of many of the amide proton resonances was lifted sufficiently to allow unambiguous observation of sequential NOE connectivities.

Not surprisingly, the helical secondary structure, defined in solution by the medium-range NOE connectivities (Fig. 4), is very similar to that found in the crystal structures of Mb (Takano, 1977a,b). The A-helix extends from Glu[4] to Ala[19], the B-helix from Val[21] to Ser[35], the C-helix from Glu[38] to Lys[42], the E-helix from Ser[58] to Lys[78], the G-helix from Ile[101] to Arg[118], and the H-helix spans residues Ala[125] to Leu[149]. Given the uncertainty in defining the ends of helices from medium-range NOE connectivities, these helices correspond closely to those defined in the X-ray structures. At first glance, the NOE data appear to indicate that the F-helix is longer in solution than in the crystal (Leu[86]–Ala[94]), since medium-range NOE connectivities extend from Leu[86] to Lys[98]. However, $d_{\alpha N}(i,i+3)$ NOEs to the amide protons of Lys[96], His[97] and Lys[98] are absent; rather, the medium-range NOE connectivities observed to these residues are $d_{\alpha N}(i,i+4)$ and $d_{\alpha N}(i,i+5)$. Thus, the F-helix in solution probably terminates at Ala[94] or Thr[95], as in the crystal, and the additional medium-range NOE connectivities extending to Lys[98] reflect the geometry of the FG loop. Indeed, these NOEs, and the $d_{NN}(i,i+2)$ connectivities observed in this region, are predicted on the basis of the X-ray coordinates. Finally, assignments have not yet been made for

the first two residues, Thr[51] and Glu[52], that begin the D-helix in the crystal structures; however, residues Ala[53] to Ala[57] exhibit NOE connectivities characteristic of a helix.

A series of medium-range $d_{\alpha N}(i,i+3)$ and $d_{\alpha N}(i,i+2)$ NOE connectivities is observed from Phe[43] to Leu[49], suggesting the presence of a short $3_{10}$-helix. This region is termed the CD loop and is not normally considered as one of the eight helices that constitute the myoglobin fold. However, examination of the hydrogen-bonding pattern in the neutron structure of MbCO (Schoenborn, 1971; Hanson and Schoenborn, 1981) reveals $3_{10}$-helical hydrogen bonds between Leu[40]-Phe[43], Phe[43]-Phe[46] and Asp[44]-Lys[47]. Given the occurrence of this irregular $3_{10}$-helix-like structure in the solid state, it is not surprising that $d_{\alpha N}(i,i+3)$ and $d_{\alpha N}(i,i+2)$ NOE connectivities are observed in solution.

## CONCLUSIONS

Using only homonuclear 2D spectra and 2D and 3D $^{15}$N-dispersed TOCSY and NOESY experiments, we have successfully assigned 95% of the backbone resonances and many of the side-chain resonances of MbCO. The observed sequential and medium-range NOE connectivities confirm that the helical secondary structure of myoglobin in solution is very similar to that observed in the crystal structures. The assignments reported in this paper have been used to obtain constraints for calculation of 3D solution structures of MbCO using distance geometry and restrained molecular dynamics, including application of a novel chemical-shift refinement procedure (Ösapay, Thériault, Wright and Case, manuscript in preparation). The resulting NMR structures are very similar to the X-ray and neutron structures of MbCO. In addition, the backbone assignments form the basis for detailed measurements of amide proton-exchange rates and for hydrogen-exchange pulse labeling studies of myoglobin folding pathways (Jennings and Wright, 1993). Future measurements of backbone dynamics and hydration are planned.

## ACKNOWLEDGEMENTS

We thank Linda Tennant for technical assistance, Jane Dyson and Pat Jennings for valuable assistance and discussions, and David Case, Klara Ösapay, Mark Rance and John Cavanagh for helpful discussions. This work was supported by grants DK34909 (to P.E.W.) and GM31756 (to S.G.S.) from the National Institutes of Health.

## REFERENCES

Balasubramanian, S., Lambright, D.G., Marden, M.C. and Boxer, S.G. (1993) *Biochemistry*, **32**, 2202–2212.

Bax, A. and Subramanian, S. (1986) *J. Magn. Reson.*, **67**, 565–569.

Bax, A., Ikura, M., Kay, L.E., Torchia, D.A. and Tschudin, R. (1990) *J. Magn. Reson.*, **86**, 304–318.

Billeter, M., Braun, W. and Wüthrich, K. (1982) *J. Mol. Biol.*, **155**, 321–346.

Brantley Jr., R.E., Smerdon, S.J., Wilkinson, A.J., Singleton, E.W. and Olson, J.S. (1993) *J. Biol. Chem.*, **268**, 6995–7010.

Braunschweiler, L., Bodenhausen, G. and Ernst, R.R. (1983) *Mol. Phys.*, **48**, 535–560.

Braunstein, D., Ansari, A., Berendzen, J., Cowen, B.R., Egeberg, K.D., Frauenfelder, H., Hong, M.K., Ormos, P., Sauke, T.B., Scholl, R., Schulte, A., Sligar, S.G., Springer, B.A., Steinbach, P.J. and Young, R.D. (1988) *Proc. Natl. Acad. Sci. USA*, **85**, 8497–8501.

Carver, T.E., Brantley Jr., R.E., Singleton, E.W., Arduini, R.M., Quillin, M.L., Phillips Jr., G.N. and Olson, J.S. (1992) *J. Biol. Chem.*, **267**, 14443–14450.

Case, D.A. and Karplus, M. (1979) *J. Mol. Biol.*, **132**, 343–368.
Chazin, W.J., Rance, M. and Wright, P.E. (1988) *J. Mol. Biol.*, **202**, 603–622.
Chiu, M.L. (1992) Ph.D. Thesis, University of Illinois, Urbana-Champaign, IL.
Dalvit, C., Rance, M. and Wright, P.E. (1986) *J. Magn. Reson.*, **69**, 356–361.
Dalvit, C. and Wright, P.E. (1987) *J. Mol. Biol.*, **194**, 313–327.
Dalvit, C., Wright, P.E. and Rance, M. (1987) *J. Magn. Reson.*, **71**, 539–543.
Davis, D.G. (1989) *J. Magn. Reson.*, **81**, 603–607.
Dodson, G., Hubbard, R.E., Oldfield, T.J., Smerdon, S.J. and Wilkinson, A.J. (1988) *Protein Eng.*, **2**, 233–237.
Driscoll, P.C., Clore, G.M., Marion, D., Wingfield, P.T. and Gronenborn, A.M. (1990) *Biochemistry*, **29**, 3542–3556.
Drobny, G., Pines, A., Sinton, S., Weitekamp, D. and Wemmer, D. (1979) *Symp. Faraday Soc.*, **13**, 49–55.
Elber, R. and Karplus, M. (1987) *Science*, **235**, 318–321.
Fesik, S.W. and Zuiderweg, E.R.P. (1990) *Q. Rev. Biophys.*, **23**, 97–131.
Frauenfelder, H., Petsko, G.A. and Tsernoglou, D. (1979) *Nature*, **280**, 558–563.
Gibson, Q.H., Regan, R., Elber, R., Olson, J.S. and Carver, T.E. (1992) *J. Biol. Chem.*, **267**, 22022–22034.
Guillemette, J.G., Matsushima-Hibiya, Y., Atkinson, T. and Smith, M. (1991) *Protein Eng.*, **4**, 585–592.
Hanson, J.C. and Schoenborn, B.P. (1981) *J. Mol. Biol.*, **153**, 117–146.
Hartmann, H., Parak, F., Steigemann, W., Petsko, G.A., Ponzi, D.R. and Frauenfelder, H. (1982) *Proc. Natl. Acad. Sci. USA*, **79**, 4967–4971.
Henry, E.R. (1993) *Biophys. J.*, **64**, 869–885.
Jennings, P.A. and Wright, P.E. (1993) *Science*, **262**, 892–896.
Kottalam, J. and Case, D.A. (1988) *J. Am. Chem. Soc.*, **110**, 7690–7697.
Kumar, A., Ernst, R.R. and Wüthrich, K. (1980) *Biochem. Biophys. Res. Commun.*, **95**, 1–6.
Kuriyan, J., Wilz, S., Karplus, M. and Petsko, G.A. (1986) *J. Mol. Biol.*, **192**, 133–154.
Lambright, D.G., Balasubramanian, S. and Boxer, S.G. (1989) *J. Mol. Biol.*, **207**, 289–299.
Levy, R.M., Sheridan, R.P., Keepers, J.W., Dubey, G.S., Swaminathan, S. and Karplus, M. (1985) *Biophys. J.*, **48**, 509–518.
Live, D.H., Davis, D.G., Agosta, W.C. and Cowburn, D. (1984) *J. Am. Chem. Soc.*, **106**, 1939–1941.
Mabbutt, B.C. and Wright, P.E. (1985) *Biochim. Biophys. Acta*, **832**, 175–185.
Marion, D. and Wüthrich, K. (1983) *Biochem. Biophys. Res. Commun.*, **113**, 967–974.
Marion, D., Driscoll, P.C., Kay, L.E., Wingfield, P.T., Bax, A., Gronenborn, A.M. and Clore, G.M. (1989a) *Biochemistry*, **28**, 6150–6156.
Marion, D., Kay, L.E., Sparks, S.W., Torchia, D.A. and Bax, A. (1989b) *J. Am. Chem. Soc.*, **111**, 1515–1517.
Norwood, T.J., Boyd, J., Heritage, J.E., Soffe, N. and Campbell, I.D. (1990) *J. Magn. Reson.*, **87**, 488–501.
Phillips Jr., G.N. (1990) *Biophys. J.*, **57**, 381–383.
Phillips Jr., G.N., Arduini, R.M., Springer, B.A. and Sligar, S.G. (1990) *Proteins*, **7**, 358–365.
Phillips, S.E.V. (1980) *J. Mol. Biol.*, **142**, 531–554.
Phillips, S.E.V. and Schoenborn, B.P. (1981) *Nature*, **292**, 81–82.
Rance, M. and Byrd, R.A. (1983) *J. Magn. Reson.*, **52**, 221–240.
Rance, M., Sørensen, O.W., Bodenhausen, G., Wagner, G., Ernst, R.R. and Wüthrich, K. (1983) *Biochem. Biophys. Res. Commun.*, **117**, 479–485.
Rance, M. and Wright, P.E. (1986) J. Magn. Reson., **66**, 372–378.
Rance, M., Chazin, W.J., Dalvit, C. and Wright, P.E. (1989) *Methods Enzymol.*, **176**, 114–133.
Schoenborn, B.P. (1971) *Cold Spring Harbor Symp. Quant. Biol.*, **36**, 569–575.
Shaka, A.J., Barker, P.B. and Freeman, R. (1985) *J. Magn. Reson.*, **64**, 547–552.
Shaka, A.J., Lee, C.J. and Pines, A. (1988) *J. Magn. Reson.*, **77**, 274–293.
Springer, B.A. and Sligar, S.G. (1987) *Proc. Natl. Acad. Sci. USA*, **84**, 8961–8965.
Takano, T. (1977a) *J. Mol. Biol.*, **110**, 537–568.
Takano, T. (1977b) *J. Mol. Biol.*, **110**, 569–584.
Varadarajan, R., Szabo, A. and Boxer, S.G. (1985) *Proc. Natl. Acad. Sci. USA*, **82**, 5681–5684.
Varadarajan, R., Lambright, D.G. and Boxer, S.G. (1989) *Biochemistry*, **28**, 3771–3781.
Wagner, G. (1983) *J. Magn. Reson.*, **55**, 151–156.